

Thermodynamic figure of merit for thermophotovoltaics

Maxime Giteau^{✉,*}, Michela F. Picardi[✉], and Georgia T. Papadakis^{✉,*}

ICFO—The Institute of Photonic Sciences, Barcelona, Spain

ABSTRACT. Comparing the performance of thermophotovoltaic (TPV) devices is challenging due to a lack of standard operation conditions. Here, we propose a universal figure of merit (FOM) that can be used to evaluate the performance of TPV devices that operate in the far-field regime relative to their thermodynamic bounds. The introduced FOM alleviates temperature dependence and accounts for the fundamental trade-off between power density and efficiency. Based on this FOM, we present a classification of TPV performances reported in recent experiments.

© 2024 Society of Photo-Optical Instrumentation Engineers (SPIE) [DOI: [10.1117/1.JPE.14.042402](https://doi.org/10.1117/1.JPE.14.042402)]

Keywords: thermophotovoltaics; thermodynamic efficiency; electrical power density; radiative heat engines

Paper 23051SSC received Nov. 24, 2023; revised Jan. 5, 2024; accepted Jan. 16, 2024; published Feb. 5, 2024.

Thermophotovoltaics (TPVs) enable the conversion of heat radiatively emitted by a hot emitter into electricity using photovoltaic (PV) cells.¹ Owing to promising applications in thermal energy storage and waste heat recovery, the field has been steadily growing, with significant performance advancements reported recently.^{2–7}

Despite this rapid progress, it remains challenging to compare the performance of TPV devices due to a lack of standard operation conditions. Indeed, depending on parameters such as the temperature and spectral emissivity of the emitter as well as the view factor of the experimental setup TPV operation can vary dramatically. Furthermore, the performance of TPV devices must be assessed with two metrics: the electrical power output density P_{el} (in W/m^2) and the pair-wise efficiency $\eta = \frac{P_{el}}{P_{el} + Q}$, where Q is the heat density (in W/m^2) lost in the PV cell.⁸ η is thermodynamically bound by the Carnot efficiency $\eta_C = 1 - T_C/T_H$, where T_C and T_H are the temperature of the cell and emitter, respectively. For systems operating in the far-field regime, P_{el} is fundamentally bound by the blackbody limit (σT_H^4), where σ is the Stefan–Boltzmann constant.

Since both efficiency and electrical power density depend on T_C and T_H , it is difficult to evaluate the performance of TPV systems operating at different temperatures. To eliminate the temperature dependence in TPV performance metrics, one may present normalized power density and efficiency: $\rho = P_{el}/\sigma T_H^4$ and η/η_C . For reference, in Fig. 1, we present the classification of recently reported TPV performances in terms of these two normalized metrics. Nonetheless, describing TPV performance in this way ignores the fundamental trade-off between both metrics.¹⁵ Importantly, although an experiment conducted with a lower view factor will present a higher TPV efficiency due to reduced ohmic losses, this comes at the cost of compromised power density and does not reflect on the real operation conditions of a TPV system.⁶

In this paper, we propose a thermodynamic figure of merit (FOM) to evaluate TPV performance based on Ref. 9, where we reported the thermodynamic performance bounds for reciprocal radiative heat engines encompassing all TPV devices to date. The introduced FOM

*Address all correspondence to Maxime Giteau, maxime.giteau.pro@gmail.com; Georgia T. Papadakis, georgia.papadakis@icfo.eu

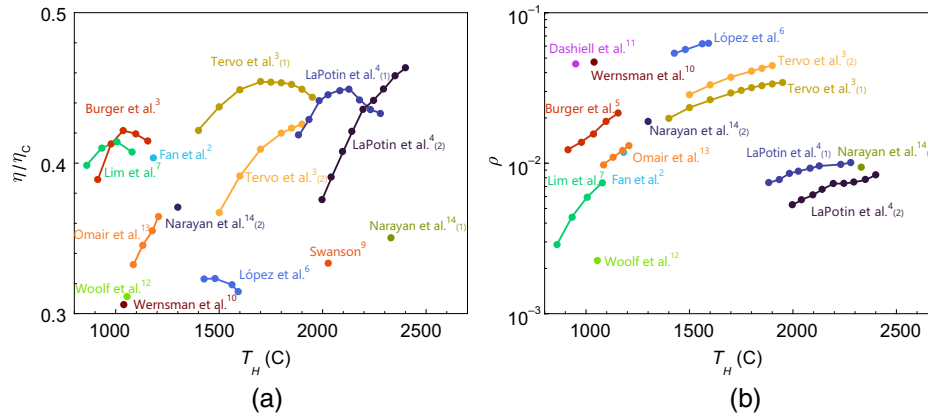


Fig. 1 (a) Efficiency normalized to the Carnot limit η/η_C and (b) electrical power output normalized to blackbody radiation ρ , as reported in different experimental works as a function of the emitter temperature. We consider $T_C = 300$ K for all cases. Reported references are Swanson⁹ (only efficiency was reported), Wernsman et al.,¹⁰ Dashiell et al.¹¹ ($\eta/\eta_C = 0.261$ so it does not appear on the graph), Woolf et al.,¹² Omail et al.,¹³ Narayan et al.,¹⁴ Fan et al.,² Tervo et al.,³ LaPotin et al.,⁴ Burger et al.,⁵ López et al.,⁶ and Lim et al.⁷ Numbers in brackets indicate different devices in the same publication.

alleviates temperature dependence, accounts for the fundamental trade-off between power density and efficiency, and quantifies how far from the thermodynamic limit a given device operates. In particular, from Ref. 9, the maximum normalized power $\rho = P_{el}/\sigma T_H^4$ achievable for a given efficiency η is well approximated by

$$\rho = \eta \left[1 - \left(\frac{T_C/T_H}{1 - \eta} \right)^4 \right]. \quad (1)$$

We note that this bound can be overcome by leveraging super-Planckian heat transfer, either via operation in the near-field regime¹⁶ or using thermophotonics.¹⁷ In both cases, radiative heat transfer can surpass the blackbody limit ($\rho > 1$), rendering Eq. (1) invalid. Here, however, we focus on conventional far-field operation and a passive emitter. In contrast, the $\rho(\eta)$ characteristic of a practical TPV system with an emitter temperature T_H and cell temperature T_C is obtained by sweeping the cell's voltage from 0 to the open-circuit voltage, forming the characteristic closed contour shown in Fig. 2 (black curve). The device's performance for this emitter temperature T_H is bounded by the thermodynamic limit given by Eq. (1) (red curve). For each (ρ, η) data point, we can calculate an effective temperature T_H^{eff} , or equivalently an effective Carnot efficiency $\eta_C^{\text{eff}} = 1 - T_C/T_H^{\text{eff}}$, using Eq. (1). The thermodynamic curve corresponding to the maximal

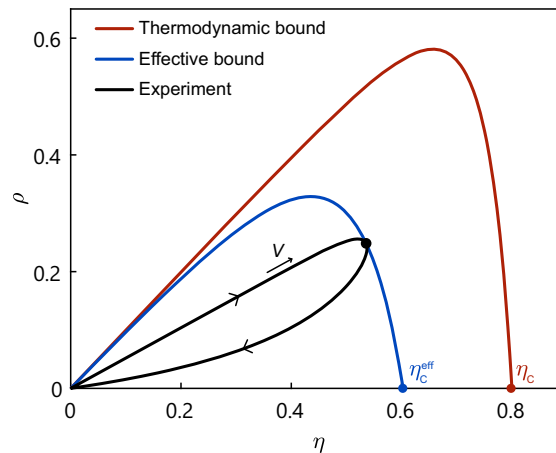


Fig. 2 Illustration of the method to determine the thermodynamic FOM for a given experiment with $T_C = 300$ K and $T_H = 1500$ K. In the case illustrated here, $\phi \approx 0.75$.

effective Carnot efficiency (blue curve) is tangential to the experimental curve at the thermodynamic optimum (black point). We define the thermodynamic FOM as the ratio between the Carnot efficiencies

$$\phi = \frac{\eta_C^{\text{eff}}}{\eta_C} \quad (2)$$

based on which we can classify TPV devices operating at different temperatures using a single metric. This thermodynamic FOM establishes a correspondence between the reported device and a thermodynamically optimal radiative heat engine operating at a lower emitter temperature T_H^{eff} . It takes values between 0 and 1, a higher value corresponding to a device operating closer to the thermodynamic limit.

Although it may appear from Eq. (2) as an efficiency metric, this thermodynamic FOM encompasses power density as well. Indeed, ϕ is always superior to η/η_C , and the difference between the two reflects on ρ . For devices with low power output ($\rho \ll \eta$), ϕ is roughly approximated by η/η_C . Using this FOM, we classify in Fig. 3 all TPV experiments, irrespective of experimental conditions. As seen when comparing Figs. 1 and 3, $\phi \approx \eta/\eta_C$ for devices with low power output ($\rho \ll \eta$). Conversely, the experiments that report the largest normalized power output to date^{6,10} show a FOM significantly higher than their normalized efficiency. Also, increasing either the power or the efficiency systematically increases the FOM. As a result, ϕ accounts for the power-efficiency trade-off associated with operating at low view factors.

In Fig. 3, we show the FOM achieved by each system as a function of temperature. Thereby, it is clear that ϕ tends to be higher for higher emitter temperatures. This is because PV cells with higher bandgaps, which tend to have lower nonradiative recombinations, are usually employed. As shown in Fig. 3, experiments remain significantly below the thermodynamic limit ($\phi = 1$). Current records are approaching $\phi \approx 0.47$ for very high emitter temperatures ($T_H > 1500^\circ\text{C}$).^{3,4} At the same time, devices operating at lower temperatures have demonstrated $\phi > 0.4$.^{2,5,7}

This FOM is a thermodynamic metric, and as such it should not be used to compare two devices optimized for different applications. Additionally, computing ϕ at the maximum power point in the characteristic curve (Fig. 2) yields a systematic but negligible underestimation of the FOM. This has no impact for practical devices that operate far from the radiative limit since their $\rho(\eta)$ characteristic is very narrow.

The introduced FOM can serve as a metric to track progress in the field of TPVs over the coming years. Indeed, as experiments get closer to the thermodynamic limits, we expect the power-efficiency trade-off to become of greater concern, making this FOM useful for performance assessment.

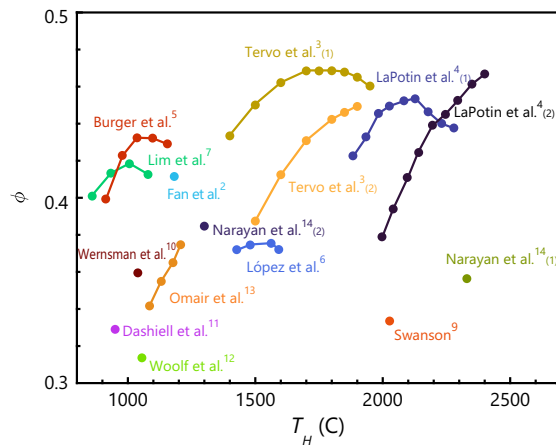


Fig. 3 Thermodynamic FOM for a set of reported experiments as a function of the emitter temperature. We consider $T_C = 300$ K for all cases. Reported references are Swanson,⁹ Wernsman et al.,¹⁰ Dashiell et al.,¹¹ Woolf et al.,¹² Omais et al.,¹³ Narayan et al.,¹⁴ Fan et al.,² Tervo et al.,³ LaPotin et al.,⁴ Burger et al.,⁵ López et al.,⁶ and Lim et al.⁷ Numbers in brackets indicate different devices in the same publication.

Disclosures

The authors declare no competing financial interest.

Code and Data Availability

All data in support of the findings of this paper are available within the article. Tabulated data can be provided upon reasonable request.

Acknowledgments

The authors thank Rodolphe Vaillon and Peter Bernel for valuable feedback. This work has been supported in part by the “la Caixa” Foundation (ID 100010434), the Spanish MICINN (PID2021-125441OA-I00, PID2020-112625GB-I00, and CEX2019-000910-S), the European Union (fellowship LCF/BQ/PI21/11830019 under the Marie Skłodowska-Curie Grant Agreement No. 847648), Generalitat de Catalunya (2021 SGR 01443), Fundació Cellex, and Fundació Mir-Puig. M.G. acknowledges financial support from the Severo Ochoa Excellence Fellowship. M.F.P. received the support of a fellowship from “la Caixa” Foundation (ID 100010434). The fellowship code is LCF/BQ/PI23/11970026.

References

1. A. Datas and R. Vaillon, “Chapter 11—Thermophotovoltaic energy conversion,” in *Ultra-High Temperature Thermal Energy Storage, Transfer and Conversion*, A. Datas, Ed., pp. 285–308, Woodhead Publishing (2021).
2. D. Fan et al., “Near-perfect photon utilization in an air-bridge thermophotovoltaic cell,” *Nature* **586**(7828), 237–241 (2020).
3. E. J. Tervo et al., “Efficient and scalable GaInAs thermophotovoltaic devices,” *Joule* **6**(11), 2566–2584 (2022).
4. A. LaPotin et al., “Thermophotovoltaic efficiency of 40%,” *Nature* **604**(7905), 287–291 (2022).
5. T. Burger et al., “Semitransparent thermophotovoltaics for efficient utilization of moderate temperature thermal radiation,” *PNAS* **119**(48), e2215977119 (2022).
6. E. López, I. Artacho, and A. Datas, “Thermophotovoltaic conversion efficiency measurement at high view factors,” *Sol. Energy Mater. Sol. Cells* **250**, 112069 (2023).
7. J. Lim et al., “Enhanced photon utilization in single cavity mode air-bridge thermophotovoltaic cells,” *ACS Energy Lett.* **8**(7), 2935–2939 (2023).
8. T. Burger et al., “Present efficiencies and future opportunities in thermophotovoltaics,” *Joule* **4**(8), 1660–1680 (2020).
9. R. M. Swanson, “Recent developments in thermophotovoltaic conversion,” in *Int. Electron Devices Meet.*, Vol. 1980, pp. 186–189 (1980).
10. B. Wernsman et al., “Greater than 20% radiant heat conversion efficiency of a thermophotovoltaic radiator/module system using reflective spectral control,” *IEEE Trans. Electron Devices* **51**(3), 512–515 (2004).
11. M. W. Dashiell et al., “Quaternary InGaAsSb thermophotovoltaic diodes,” *IEEE Trans. Electron Devices* **53**(12), 2879–2891 (2006).
12. D. N. Woolf et al., “High-efficiency thermophotovoltaic energy conversion enabled by a metamaterial selective emitter,” *Optica* **5**(2), 213–218 (2018).
13. Z. Omair et al., “Ultraefficient thermophotovoltaic power conversion by band-edge spectral filtering,” *PNAS* **116**(31), 15356–15361 (2019).
14. T. C. Narayan et al., “World record demonstration of >30% thermophotovoltaic conversion efficiency,” in *47th IEEE Photovoltaic Specialists Conf. (PVSC)*, pp. 1792–1795 (2020).
15. M. Giteau, M. F. Picardi, and G. T. Papadakis, “Thermodynamic performance bounds for radiative heat engines,” *Phys. Rev. Appl.* **20**(6), L061003 (2023).
16. M. Laroche, R. Carminati, and J.-J. Greffet, “Near-field thermophotovoltaic energy conversion,” *J. Appl. Phys.* **100**(6), 063704 (2006).
17. N.-P. Harder and M. A. Green “Thermophotonics,” *Semicond. Sci. Technol.* **18**(5), S270 (2003).

Maxime Giteau is a postdoctoral research fellow at ICFO, Barcelona, Spain. He received his MSc degrees in engineering and solid state physics, respectively, from ISAE Supaero and Paul Sabatier University, France, in 2016, and his PhD from the University of Tokyo in 2020. His research focuses on energy conversion based on radiative heat transfer, including the spectral and directional engineering of thermal emission, the thermodynamics of radiative heat engines, and the design of high-performance photovoltaic devices.

Michela F. Picardi is a postdoctoral research fellow at ICFO, Barcelona, Spain. She received her PhD in physics from King's College London in 2020 and is currently a "la Caixa" Junior Leader Fellow at ICFO. Her research interests include fundamental properties of light at the nanoscale, near-field radiative heat transfer, and engineering of directionality and topologically protected modes via nanostructures and resonators.

Georgia T. Papadakis is a professor and group leader at ICFO, Barcelona, Spain. She received her PhD in applied physics from Caltech in 2018 and carried out her postdoctoral studies in the Tomkat Center for Renewable Energy at Stanford University (2018–2021). Her group's work focuses on thermal photonics, the control of thermal radiation in the far-field and near-field regime, as well as novel concepts in heat-to-electricity energy conversion.